http://dx.doi.org/10.11142/jicems.2013.2.2.165
Journal of International Conference on Electrical Machines and Systems Vol. 2, No. 2, pp. 165~170, 2013 **165**

Iron Loss Analysis of a Permanent Magnet Rotating Machine Taking Account of the Vector Hysteretic Properties of Electrical Steel Sheet

Heesung Yoon *, Seok-Myeong Jang ** and Chang Seop Koh *

Abstract – This paper presents the iron loss prediction of rotating electric machines taking account of the vector hysteretic properties of electrical steel sheet. The E&S vector hysteresis model is adopted to describe the vector hysteretic properties of a non-oriented electrical steel sheet, and incorporated into finite element analysis (FEA) for magnetic field analysis and iron loss prediction. A permanent magnet synchronous generator is taken as a numerical model, and the analyzed magnetic field distribution and predicted iron loss by using the proposed method is compared with those from a conventional method which employs an empirical iron loss formula with FEA based on a non-linear *B-H* curve. Through the comparison the effectiveness of the presented method for the iron loss prediction of the rotating machine is verified.

Keywords: E&S vector hysteresis model, Finite element method, Synchronous generator

1. Introduction

There is increasing demands to develop high-efficiency rotating electric machines to reduce energy consumption. In order to meet the demands, it is essential to predict the iron loss accurately at the design stage because the iron loss is of great importance in the total energy loss. The iron loss from rotating magnetic fields is in general significantly bigger than that from alternating ones even at the same magnitude of magnetic flux density, and accordingly its precise prediction is essential in the estimation of iron loss of rotating electrical machines [1]. The rotational iron loss, however, involves complicated vector hysteretic properties of an electrical steel sheet (ESS), and its precise prediction still remains complex and arduous works [2].

Conventionally the rotational iron loss has been estimated by using empirical iron loss formula based on Steinmetz equation [3]-[6]. In these researches, both the hysteresis and eddy current losses are calculated from the magnetic field distribution obtained by using FEA which utilizes a single non-linear *B-H* curve ignoring the vector hysteretic properties of ESS. Especially, the iron loss for an arbitrary rotating *B*-waveform is commonly estimated taking into account the ratio of minor to major axis of the approximated elliptic *B*-waveform with different coefficients of the Steinmetz equation from those for alternating *B*-waveform. Even if the empirical formula may estimate the rotational iron loss correctly, these methods have obvious error because of the exclusion of the vector hysteretic properties of ESS at the magnetic field analysis [7].

Recently vector hysteresis models such as Jiles-Atherton model [7], vector Preisach model [8], vector play model [9] and E&S (Enokizono&Soda) model [10]-[12] have been developed to directly describe the vector hysteretic properties of ESS, and combined with FEA to be applied for magnetic field and iron loss analyses of electric machines. These methods commonly calculate the iron loss directly from the *B*- and its corresponding *H*-waveforms instead of using an empirical formula. Among them, E&S model is an attractive engineering model because it gives more accurate iron losses under not only the alternating but also the rotating magnetic fields than the others [10]-[11]. For precise iron loss prediction under distorted magnetic field, recently, the dynamic E&S model is suggested by improving eddy current term and coefficient calculation algorithm [12], [13].

In this paper, the E&S vector hysteresis model is combined with FEA and applied to the analysis of the iron loss of a permanent magnet synchronous generator (PMSG).

---

* College of Electrical & Computer Engineering, Chungbuk National University, Korea. (kohcs@chungbuk.ac.kr)

** Department of Electrical Engineering, Chungnam National University, Korea. (smjang@cnu.ac.kr)

Received 14 May 2013 ; Accepted 23 May 2013

2. Vector Hysteretic Properties of Non-oriented Electrical Steel Sheet

In order to measure the vector hysteretic properties of a non-oriented ESS (35PN440), a two-dimensional single sheet tester (2-D SST) developed in [14] is used. The *H*-waveforms corresponding to arbitrary elliptic *B*-waveforms with geometric parameters, $B_{\max}$, α and φ, defined in Fig. 1 are measured at 50Hz adopting *B*-waveform control.

Fig. 2 shows the *H*-waveforms measured under rotating *B*-waveforms. Even though the *B*-waveforms are purely circular, the corresponding *H*-waveforms are far from circular. The magnitude of *H* along the transverse direction (TD) is significantly larger than that along the rolling direction (RD) due to the anisotropic property of the non-oriented ESS. It is found that, in Fig. 2(d), there are phase differences between *B*- and *H*-vectors, and moreover they do not remain a constant with respect to the rotation of the *B*-vector.

Fig. 3 compares the measured iron losses according to the variations of $B_{\max}$ and α when φ is equal to zero. It can be seen that the iron loss by rotating magnetic field (α=1) is considerably larger than that by alternating one (α=0) at the same $B_{\max}$. For example, at 1.2T of maximum magnetic flux density, the rotating magnetic field gives 87% more iron loss (2.37W/kg) than alternating one (1.27W/kg).

The above magnetic properties and iron loss characteristics come from the vector hysteretic properties of the ESS, and cannot be described precisely via the conventional method using empirical iron loss formula and FEA with non-linear *B*-*H* curve [3]-[6].

3. Iron Loss Prediction using FEA combined with E&S Vector Hysteresis Model

In order to describe the vector hysteretic properties, in this paper, the E&S vector hysteresis model is adopted. The E&S model defines the relationship between *B*- and *H*-waveforms as follows [10]-[12]:

$$H_k(\tau)=\nu_k B_k(\tau)+h_k\frac{\partial B_{k1}(\tau)}{\partial \tau}+\frac{\sigma\omega d^2}{12}\frac{\partial B_k(\tau)}{\partial \tau} \qquad (1)$$
$$k=R,T \text{ and } \tau=\omega t\in[0,2\pi]$$

where the subscripts *R* and *T* denote RD and TD of the ESS, respectively, ν_k and h_k are the magnetic reluctivity and hysteresis coefficients, respectively, ω is the angular frequency of the fundamental component of the *B*-waveform, B_1 is the fundamental component of the *B*-waveform, σ and *d* are the conductivity and thickness of the ESS, respectively.

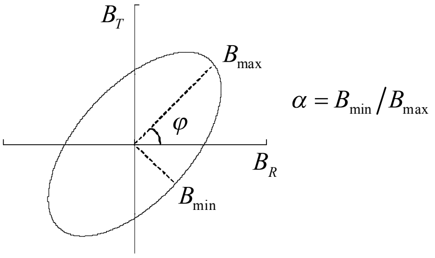

Fig. 1. Definition of *B*-waveform using $B_{\max}$, φ and α

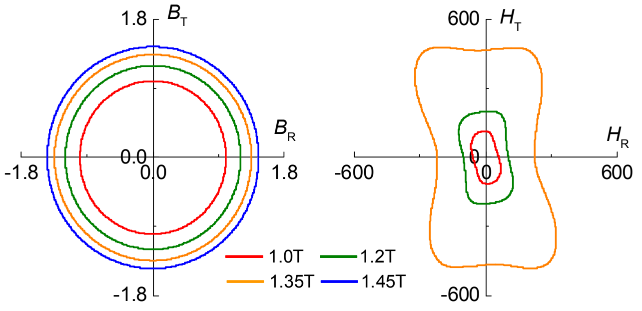

(a) *B*-waveforms (b) *H*-waveform (1.0~1.35T)

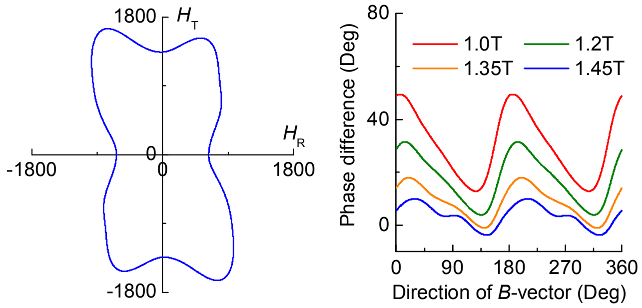

(c) *H*-waveform (1.45T) (d) phase difference

Fig. 2. Measured *H*-waveforms under rotating magnetic flux densities with variation of $B_{\max}$

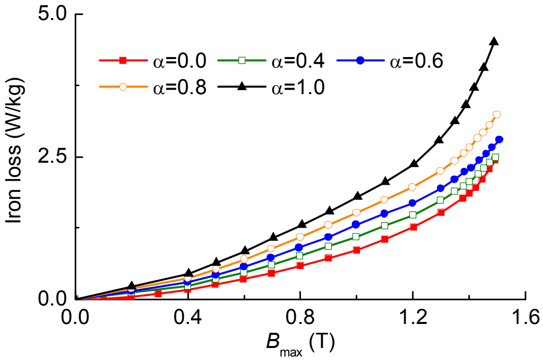

Fig. 3. Comparison of measured iron losses according to variations of $B_{\max}$ and α when φ=0°

The reluctivity and hysteresis coefficients in (1) are calculated by experimental data measured from the 2-D SST under various elliptic *B*-waveforms defined in Fig. 1 [11],

[14].

The governing equation incorporated with the E&S model is derived from Maxwell's equations as follows [12]:

$$\nabla\times\left(\mathbf{v}\nabla\times\mathbf{A}+\mathbf{h}\frac{\partial\mathbf{B}_1}{\partial\tau}+\frac{\sigma\omega d^2}{12}\frac{\partial\left(\nabla\times\mathbf{A}\right)}{\partial\tau}\right)=\mathbf{J}_0 \qquad (2)$$

where **A** and $\mathbf{J}_0$ are vector magnetic potential and applied current density, respectively.

By solving the governing equation by means of finite element method (FEM), the local *B*-waveforms in the electrical machine are obtained, and then the corresponding *H*-waveforms can be calculated by using the E&S model of (1). The resultant iron loss is predicted directly from calculated B- and H-waveforms as follows [12]:

$$P=\frac{1}{\rho T}\int_0^T\left(H_x\frac{\partial B_x}{\partial\tau}+H_y\frac{\partial B_y}{\partial\tau}\right)d\tau \quad [W/kg] \qquad (3)$$

where ρ is the mass density, T is the exciting period.

4. Numerical Results in Permanent Magnet Rotating Machine

A permanent magnet synchronous generator shown in Fig. 4 is taken as a numerical model. The synchronous generator is made of a non-oriented ESS (35PN440), and is assembled so that RD of the stator core coincides with x-axis. Table 1 shows the specification of the synchronous generator.

In order to investigate the influence of the vector hysteretic properties of the ESS, the following conventional method considering the rotational iron loss is compared [5].

$$\begin{aligned} P&=P_{hys-alt}+P_{eddy-alt}+P_{add-rot} \quad [W/kg] \\ P_{add-rot}&=\gamma\frac{B_{\min}}{B_{\max}}\left(P_{hys-alt}+P_{eddy-alt}\right) \\ &=\gamma\alpha\left(P_{hys-alt}+P_{eddy-alt}\right) \end{aligned} \qquad (4)$$

where $P_{\text{hys-alt}}$ and $P_{\text{eddy-alt}}$ is the hysteresis and eddy current losses under alternating magnetic field, respectively, $P_{\text{add-rot}}$ is the additional iron loss caused by rotating magnetic field. The γ presents the rate of iron loss increment under rotating magnetic field to alternating iron loss, and may depend on ($B_{\max}$, φ, α) of the B-waveform. For simplicity, in this paper, the γ is fixed to 0.87 obtained from the ratio of the rotational to alternating iron losses at $B_{\max}$=1.2T shown in Fig. 3. The iron loss formula in (4) is expressed by considering both rotating magnetic field and flux density harmonics as follows [5]:

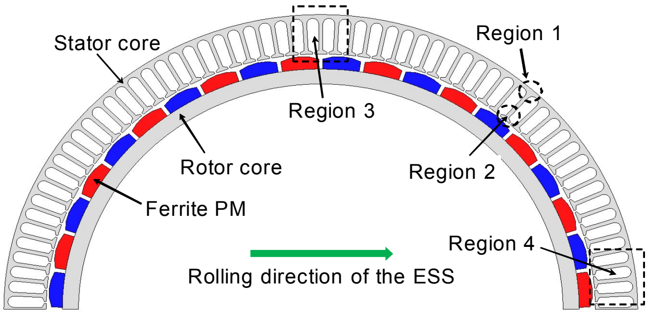

Fig. 4. A permanent magnet synchronous generator (half model)

Table 1. Specification of permanent magnet synchronous generator

	Item	Value
Stator and rotor	Rated power (W)	400
	Rated speed (rpm)	150
	Number of phases and slots	3, 120
	Electrical steel sheet	35PN440
	Outer, inner radiuses of stator (mm)	157, 136
	Outer, inner radiuses of rotor (mm)	128, 120
	Thickness of return yoke (mm)	2
	Thickness of tooth (mm)	2
	Lamination (mm)	101
	Air-gap length (mm)	1
PM	Material	Ferrite
	Residual B (T)	0.4
	Coercive force (kA/m)	318.3
	Magnetization pattern	Parallel
	Width and thickness (mm)	18.5, 7
	Number of poles	40

$$\begin{aligned} P_{hys-alt}+P_{eddy-alt}&=\sum_n\left[k_h\left(nf\right)B_{mn}^{\delta}+k_e\left(nf\right)^2B_{mn}^2\right] \\ P&=\sum_n\left[k_h\left(nf\right)B_{mn}^{\delta}+k_e\left(nf\right)^2B_{mn}^2\right]\left(1+\gamma\alpha_n\right) \end{aligned} \qquad (5)$$

where δ is a Steinmetz constant, k_{h} and k_{e} are the hysteresis and eddy current coefficients fitted from measured alternating iron loss in Fig. 3, respectively, n is harmonic order of the B-waveform, B_{mn} and α_{n} are the magnitude and axis ratio of the n-th harmonic component of the B-waveform, respectively.

Fig. 5 shows the *B*- and *H*-loci calculated by the proposed method in the region 1 and 2 of the stator core defined in Fig. 4. It is found that the rotating magnetic fields

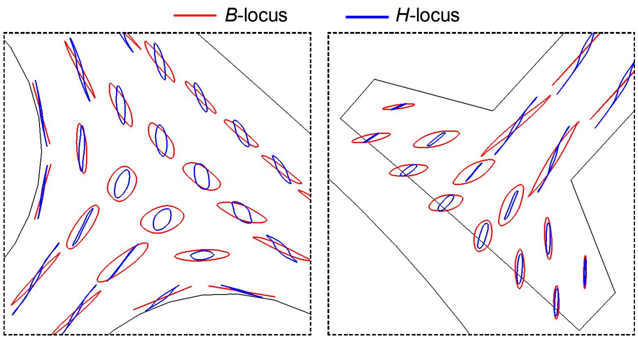

(a) region 1 (b) region 2

Fig. 5. *B* and *H*-loci, calculated by the proposed method, in the stator core

are distributed extensively in the return yoke and pole shoe of the stator core, and it is indicated that the rotational iron loss is of great importance to total iron loss in the stator core.

Fig. 6 and 7 compare the distributions of maximum magnetic flux densities ($B_{\max}$) and maximum magnetic field intensities ($H_{\max}$), calculated by the proposed and conventional methods. The conventional method gives same $H_{\max}$ distributions in the region 3 and 4 due to same $B_{\max}$ distributions. On the other hand, the proposed method gives higher $H_{\max}$ distributions in the region 3 than the region 4, especially at the stator teeth. This phenomenon results from the anisotropic magnetic property of the non-oriented ESS, and cannot be described precisely by the single non-linear *B-H* curve in the conventional method.

Fig. 8 compares the iron loss distributions calculated by the proposed and conventional methods. The following differences can be found in the iron loss distributions: 1) While the conventional method gives symmetrical loss distributions between the region 3 and 4, the proposed method gives asymmetric iron loss distributions, especially in the stator teeth. It is because that, the iron loss caused by the magnetic flux along the TD is considerably bigger than that cause by the magnetic flux along the RD due to the anisotropic magnetic properties [2]. 2) The rotational iron losses may be distributed in the re-turn yoke and pole shoe of the stator core where the rotating magnetic fields are existed as shown in Fig. 5. In the return yoke with the rotating fields of $\alpha > 0.8$, the conventional method gives similar rotational iron losses with the proposed one by the help of the γ. However, the large deviations of the rotational iron losses are observed in the pole shoe with the rotating fields of $\alpha < 0.8$. It means that, even if the conventional method adopts the additional term for the rotational iron loss, it still cannot predict precisely the rotational iron losses corresponding to various elliptic *B*-waveforms.

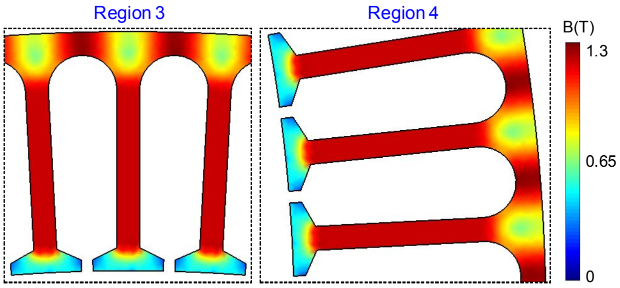

(a) conventional method

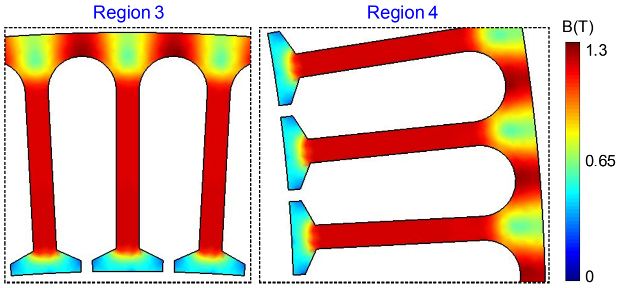

(b) proposed method

Fig. 6. Maximum magnetic flux densities calculated by the conventional and proposed methods in the stator core

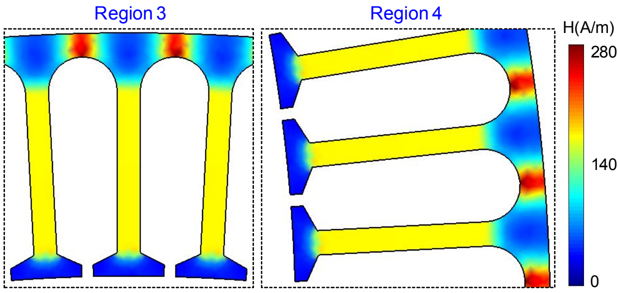

(a) conventional method

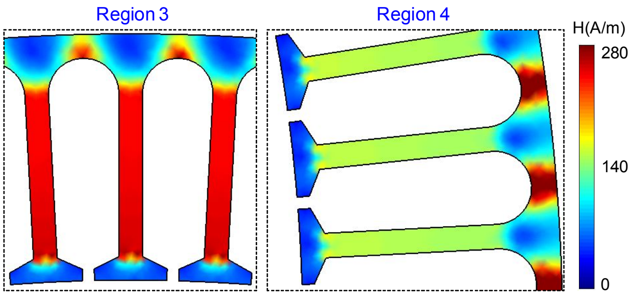

(b) proposed method

Fig. 7. Maximum magnetic field intensities calculated by the conventional and proposed methods in the stator core

For the total iron loss generated in the stator core, the pro-posed method gives 129% higher iron loss (7.35W) than the conventional one (3.2W). It is thought that this large deviation comes from that of the rotational iron loss in the pole shoe and the alternating iron loss at the stator teeth

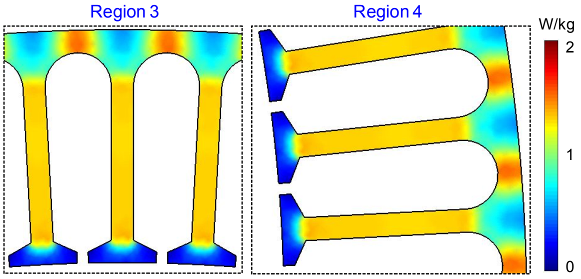

(a) conventional method

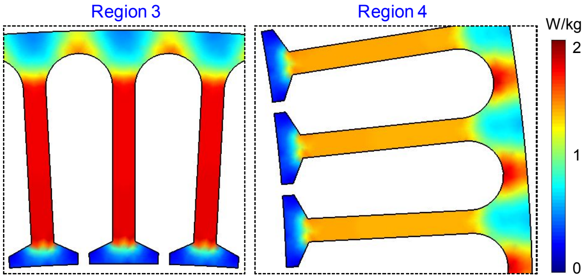

(b) proposed method

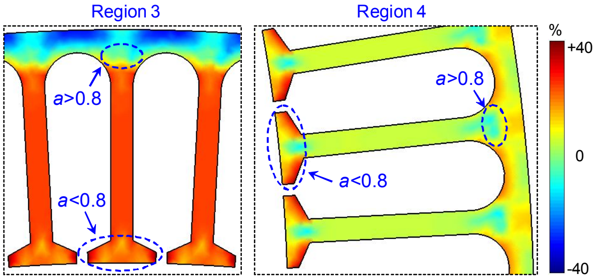

(c) percentage error between two approaches

Fig. 8. Iron losses calculated by the conventional and proposed methods in the stator core

along the TD.

5. Conclusion

In this paper, the proposed method based on the E&S vector hysteresis model is presented for the iron loss prediction of the permanent magnet rotating machine. The proposed method gives relatively higher rotational iron loss in the pole shoe and alternating one in the stator teeth along the TD than the conventional method based on the empirical iron loss formula. In consideration of the iron loss characteristics measured by the 2-D SST, it is thought that the proposed method gives more reasonable result for both not only alternating but also rotational iron losses.

Acknowledgements

This work was supported by the Human Resources Development program (No.20124030200090) of the Korea Institute of Energy Technology Evaluation and Planning (KETEP) grant funded by the Korea government Ministry of Trade, Industry and Energy.

References

[1] A. J. Moses, "Importance of rotating losses in rotating machines and transformers," *J. Maert. Eng. Perf.*, vol. 1, no. 2, pp. 235-244, 1992.

[2] M. Enokizono, T. Suzuki, and J. D. Sievert, "Measurement of iron loss using rotational magnetic loss measurement apparatus," *IEEE Transl. J. Magn. Jpn.*, vol. 6, no. 6, pp. 508-514, Jun. 1991.

[3] G. Bertotti, et al., "An improved estimation of iron losses in rotating electrical machines," *IEEE Trans. Magn.*, vol. 27, no. 6, pp. 5007-5009, Nov. 1991.

[4] J. G. Zhu and V. S. Ramsden, "Improved formulations for rotational core losses in rotating electrical machines, " *IEEE Trans. Magn.*, vol. 34, no. 4, pp. 2234-2242, Jul. 1998.

[5] L. Ma, M. Sanada, S. Morimoto, and Y. Takeda, "Prediction of iron loss in rotating machines with rotational loss included," *IEEE Trans. Magn.*, vol. 39, no. 4, pp. 2036-2041, Jul. 2003.

[6] H. Domeki, et al., "Investigation of benchmark model for estimating iron loss in rotating machines," *IEEE Trans. Magn.*, vol. 40, no. 2, pp. 794-797, Mar. 2004.

[7] J. Saitz, "Computation of the core loss in an induction motor using the vector Preisach hysteresis model incorporated in finite element analysis," *IEEE Trans. Magn.*, vol. 36, no. 4, pp. 769-773, Jul. 2000.

[8] M. V. Ferreira da Luz, J. V. Leite, A. Benabou, and N. Sadowski, "Three-phase transformer modeling using a vector hysteresis model and including the eddy current and the anomalous losses," *IEEE Trans. Magn.*, vol. 46, no. 8, pp. 3201-3204, Aug. 2010.

[9] T. Matsuo and M. Miyamoto, "Dynamic and anisotropic vector hysteresis model based on isotropic vector play model for nonoriented silicon steel sheet," *IEEE Trans. Magn.*, vol. 48, no. 2, pp. 215-218, Feb. 2012.

[10] M. Enokizono and H. Shimoji, "Vector magneto-hysteretic engineering model," *J. Mater. Process.* Tech., vol. 161, pp. 136-140, 2005.

[11] M. Song, H. Yoon, H. Yang, and C. S. Koh, "A generalized Chua-type vector hysteresis model for both the non-oriented and grain-oriented electrical steel sheet," *IEEE Trans. Magn.*, vol. 47, no. 5, pp. 1146-1149, May 2011.

[12] H. Yoon, M. Song, I. Kim, P. S. Shin, and C. S. Koh, "Accuracy improved dynamic E&S vector hysteresis model and its application to analysis of iron loss distribution in a three-phase induction motor," *IEEE Trans. Magn.*, vol. 48, no. 2, pp. 887-890, Feb. 2012.

[13] M. Enokizono, T. Todaka, and S. Urata, "Dynamic vector magneto-hysteretic E&S model considering eddy current effect," *COMPEL*, vol. 28, no. 1, pp. 85-97, 2009.

[14] Y. H. Eum, S. K. Hong, P. S. Shin, and C. S. Koh, "Measurement of two dimensional magnetic properties of electrical steel sheets under rotating magnetic fields," *The Trans. of KIEE*, vol. 55-B, no. 12, pp. 617-622, Dec. 2006.

Heesung Yoon received the B.S., M.S. and Ph. D. degrees in the department of electrical and electronics engineering, Chungbuk National University in 2005, 2007 and 2012. He is currently working in Chunbuk National University as a Post Doctor. His research interests include numerical analysis of electromagnetic fields considering vector hysteresis properties of electrical steel sheet. He can be contacted at hsyoon@chungbuk.ac.kr, (telephone) +82-43-274-2426, and (fax) +82-43-274-2426.

Seok-Myeong Jang received the B.S., M.S. and Ph.D. degrees in electrical engineering from Hanyang University, Seoul, South Korea, in 1976, 1978 and 1986 respectively. He joined the Chungnam national University in1978 and is currently a full professor of the Department of Electrical Engineering. He was a vice-chairman of Korean institute of electrical engineering (KIEE) and chairman of electric machines and energy conversion system field in KIEE from 2004 to 2005. His main research interests include electric machine design and analysis for high-speed motor system, magnetic levitation train, and renewable energy system such as wind power generation and flywheel energy storage system.

Chang Seop Koh received his B.S., M.S., and Ph. D. degrees in Electrical Engineering from Seoul National University, Seoul, Korea, in 1982, 1986, and 1992, respectively. He was visiting Professor at the Department of Electrical and Computer Engineering, Florida International University, Florida, USA, and at the Department of Electrical and Computer Engineering, Texas A&M University, Texas, USA, from May 1993 to April 1994, and from February 2003 to January 2004, respectively. He was also a Senior Researcher at the Central Research Institute of Samsung Electro- Mechanics Co., Ltd., from May 1994 to August 1996. He has been a Professor with the School of Electrical and Computer Engineering, Chungbuk National University, Korea, since 1996. His research interests include electric machine design, numerical analysis of electric machines using the finite element and boundary element methods, and optimization. He can be contacted at kohcs@chungbuk.ac.kr, (telephone) +82-43-261-2426, and (fax) +82-43-274-2426.